PNAS RESEARCH ARTICLE | NEUROSCIENCE

Head-to-head comparison of brain-derived pTau217 and total pTau217 for brain amyloid and tau pathology classification

Yuanbing Jiang[a,b,1], Wenyue Zheng[a,b,1], Zengjie Xia[a], Wan Wa Wong[a], Lily K. W. Cheng[a,b], Fanny C. Ip[a,b,c], Siu Man Choi[d], Andrew L. T. Chan[d], Ching Yu Lam[e], Ka Shing Ho[f], Chun Keung Shum[f], Jacqueline K. Y. Yuen[g], Yat Fung Shea[g], Hok Man Wai[h], Vincent C. T. Mok[i,j], Timothy C. Y. Kwok[j], Kin Y. Mok[a,b,k], Hiu Yi Wong[a,b], Henrik Zetterberg[b,k,l,m,n,o,p,q], Amy K. Y. Fu[a,b,c,r], and Nancy Y. Ip[a,b,c,r,2]

Affiliations are included on p. 9.

Contributed by Nancy Y. Ip; received December 17, 2025; accepted January 18, 2026; reviewed by Sam Gandy and Virginia M. Lee

Phosphorylated-tau 217 (pTau217) is currently the most promising blood-based biomarker for accurately detecting Alzheimer's disease (AD) pathology. However, interference from peripheral tau species in the kidneys or peripheral nerves can hinder diagnostic precision. Recently developed brain-derived pTau217 (BD-pTau217) assays emerge as highly specific tools for detecting AD-related pathological changes in the brain. In this study, we conducted a head-to-head comparison of the NULISAqpcr BD-pTau217 assay and Simoa ALZpath total p-Tau217 assay in two independent, amyloid-PET–characterized Chinese cohorts. Our results demonstrate a strong correlation between BD-pTau217 and total pTau217 (ρ = 0.89 to 0.90), with BD-pTau217 showing significantly reduced interference from kidney dysfunction, as evidenced by weaker associations with blood levels of urea ($\rho_{\text{BD-pTau217}}$ = 0.02 to 0.06, $\rho_{\text{Total-pTau217}}$ = 0.06 to 0.12) and creatinine ($\rho_{\text{BD-pTau217}}$ = 0.03 to 0.08, $\rho_{\text{Total-pTau217}}$ = 0.16 to 0.18). Moreover, BD-pTau217 is more strongly associated with amyloid-PET Centiloid values ($\rho_{\text{BD-pTau217}}$ = 0.78 to 0.80, $\rho_{\text{Total-pTau217}}$ = 0.74 to 0.77) and exhibits superior classification performance for amyloid-β (Aβ) pathology (area under the curve $[\text{AUC}]_{\text{BD-pTau217}}$ = 0.96 to 0.98, $\text{AUC}_{\text{Total-pTau217}}$ = 0.94 to 0.97). Furthermore, BD-pTau217 outperforms total pTau217 for identifying tau-positive individuals within the Aβ-positive group ($\text{AUC}_{\text{BD-pTau217}}$ = 0.89, $\text{AUC}_{\text{Total-pTau217}}$ = 0.78), facilitating more accurate disease staging. These findings underscore BD-pTau217 as a highly sensitive and specific blood-based biomarker for AD that has significant potential for early detection, precise classification, and staging of AD-related brain pathology in clinical practice.

Alzheimer's disease | tau pathology | disease staging | brain-derived pTau217 | blood biomarkers

Significance

This study demonstrates that brain-derived pTau217 (BD-pTau217) is a highly sensitive and specific blood biomarker for Alzheimer's disease (AD), effectively addressing the limitations of existing pTau217 assays, which are confounded by peripheral tau sources and kidney dysfunction. Our direct comparison of BD-pTau217 with total pTau217 in amyloid-positron emission tomography (PET)–characterized cohorts shows that BD-pTau217 offers superior accuracy for detecting early amyloid pathology and staging tau-related disease progression. These findings underscore the clinical utility of BD-pTau217 for reliable AD diagnosis and monitoring, with the potential to replace invasive and costly procedures, such as PET imaging and cerebrospinal fluid testing. The adoption of BD-pTau217 could significantly enhance early intervention, disease management, and patient outcomes in AD.

Blood-based biomarkers are increasingly recognized as valuable tools for diagnosing and prognosing Alzheimer's disease (AD), owing to their noninvasiveness, cost-effectiveness, accessibility, and accuracy (1, 2). These advantages are contributing to their growing acceptance as reliable indicators of AD pathology (2, 3). Among them, tau phosphorylated at threonine 217 (pTau217) stands out as one of the most promising fluid biomarkers for AD. Numerous studies showed that elevated levels of pTau217 in cerebrospinal fluid and plasma robustly reflect AD-related brain amyloid-beta (Aβ) and tau pathologies, demonstrating high diagnostic accuracy for distinguishing AD from other neurodegenerative diseases (1–3). Plasma pTau217 is strongly correlated with amyloid-PET and tau-PET imaging, and can identify AD at early, preclinical stages, with validated performance across diverse cohorts and ethnic groups (1, 4). Together with several available immunoassays for clinical and research applications, pTau217 is positioned as a leading candidate for noninvasive screening and staging of AD pathology (1, 3, 5).

Despite these successes, a major challenge remains regarding the specificity of plasma pTau217 for brain-derived pathology. Recent studies report that pTau217 and pTau181 levels are elevated in the blood of patients with amyotrophic lateral sclerosis (ALS); such elevation is associated with lower motor neuron dysfunction and may be due to degenerating peripheral nerves and denervated muscle fibers (6–8). Furthermore, the peripheral nervous system (PNS) and central nervous system (CNS) express structurally distinct forms of tau, with the PNS expressing a high-molecular-weight (HMW, 110 kDa) isoform and the CNS predominantly expressing six low-molecular-weight (LMW, 37 to 46 kDa) isoforms (8–10). Notably, most available immunoassays for pTau quantification, such as the Simoa ALZpath total p-Tau217 assay, recognize N-terminal epitopes present in both CNS and PNS tau; thus, they measure the total pTau217 and cannot distinguish between these isoforms (8, 11). This lack of specificity can confound measurements in conditions involving peripheral tau release, including non-AD neurodegenerative diseases such as

[1]Y.J. and W.Z. contributed equally to this work.

[2]To whom correspondence may be addressed. Email: boip@ust.hk.

This article contains supporting information online at https://www.pnas.org/lookup/suppl/doi:10.1073/pnas.2536792123/-/DCSupplemental.

Published March 2, 2026.

ALS and even kidney dysfunction (8, 12), ultimately diminishing the diagnostic accuracy of pTau217 for AD. Given this limitation, there is an urgent need for assays that selectively measure brain-derived pTau217 (BD-pTau217) to enhance the reliability of plasma biomarkers for AD pathology.

Recent advances aiming to address this issue have led to the development of assays targeting CNS-specific tau isoforms. For example, the BD-tau assay selectively measures LMW tau isoforms and serves as an indicator of neurodegeneration intensity in AD (13, 14). Moreover, the pTau217 assay developed by Lilly employs detection antibodies that target the amino acids 111 to 130, which are exclusive to the LMW tau isoforms expressed in the CNS, thereby offering improved specificity for brain-derived tau species (8). Similarly, the recently developed NULISAqpcr BD-pTau217 assay utilizes detection antibodies that target the LMW-specific region to quantify BD-pTau217 in small volumes of plasma via qPCR (Fig. 1*A*). Based on these innovations, we hypothesized that a BD-pTau217 assay designed to target CNS-specific tau isoforms, would provide superior specificity and diagnostic performance for AD-related brain pathology compared to assays that measure total pTau217.

Accordingly, in this study, we performed a head-to-head comparison of BD-pTau217 and total pTau217 in classifying brain amyloid and tau pathology across two independent cohorts. Our results demonstrate a strong correlation between BD-pTau217 and total pTau217 levels; however, BD-pTau217 exhibits less interference from kidney dysfunction and shows a stronger association with brain amyloid pathology as assessed by amyloid-PET Centiloid. Furthermore, BD-pTau217 outperforms total pTau217 for differentiating individuals with Aβ pathology from those without, and more accurately identifies tau pathology positivity among $A\beta^{+}$ individuals. Collectively, these findings suggest that BD-pTau217 may enhance diagnostic accuracy for detecting and staging AD-related brain pathology, paving the way for the development of a highly specific and sensitive diagnostic tool for AD classification and staging in clinical settings.

Results

Participant Characteristics. To conduct the head-to-head comparison of the BD-pTau217 and total pTau217 assays, we recruited a total of 429 participants (mean [SD] age, 72.78 [7.64] years; 242 females [56.64%]) from two independent, amyloid-PET–characterized Hong Kong Chinese cohorts: the discovery cohort (n = 283) and the validation cohort (n = 146). We classified participants into three groups according to their Aβ pathology status, assessed by amyloid-PET imaging and CL quantification: no or low Aβ (CL < 10, $A\beta^{Low}$), intermediate Aβ (CL 10 to 30, $A\beta^{Int}$), or high Aβ (CL > 30, $A\beta^{High}$). The discovery cohort included 283 participants (mean [SD] age, 73.86 [8.09] years; 158 females [55.83%]), including 137, 14, and 132 in the $A\beta^{Low}$, $A\beta^{Int}$, and $A\beta^{High}$ groups, respectively. Meanwhile, the validation cohort consisted of 146 participants (mean [SD] age, 70.67 [6.22] years; 84 females [57.53%]), including 79, 15, and 52 in the $A\beta^{Low}$, $A\beta^{Int}$, and $A\beta^{High}$ groups, respectively. Moreover, all participants in the validation cohort also had Tau pathology status assessed by Tau-PET imaging (Table 1).

Associations of Plasma Levels of BD-pTau217 and Total pTau217 with Kidney Function. Both the NULISAqpcr BD-pTau217 and Simoa ALZpath p-Tau217 assays employ pTau217 specific capturing antibodies but use distinct detection antibodies targeting different sites and tau isoforms (Fig. 1*A*). The NULISAqpcr BD-pTau217 assay detects tau in a region at amino acids near the exon 4 to 5 junction, characteristic of brain-derived LMW tau that skips

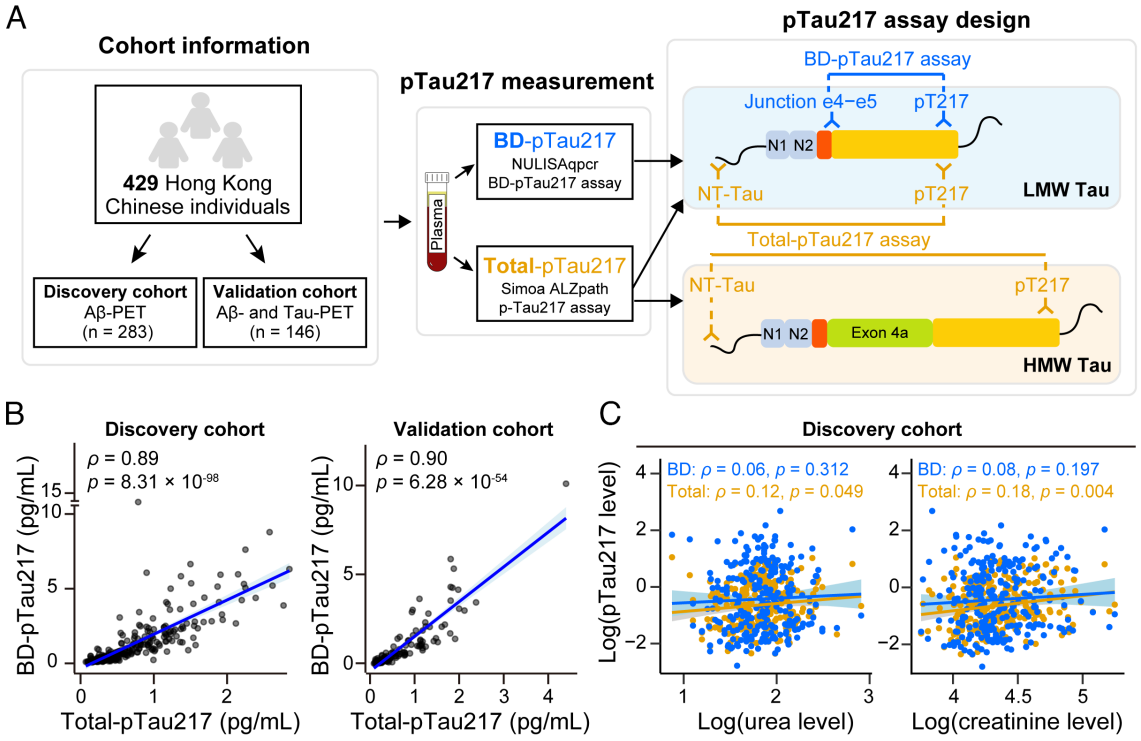

Fig. 1. Designs of the BD-pTau217 and total-pTau217 assays and their associations with renal function markers. (*A*) Schematic representation of the study workflow and assay designs, illustrating the differences in the capture methods and detection sites between the two pTau217 assays for measuring high–molecular-weight (HMW) and/or low–molecular-weight (LMW) tau species. (*B*) Correlation between the two pTau217 assays in the Discovery cohort (*Left*; n = 283) and Validation cohort (*Right*; n = 146). (*C*) Scatter plots showing the correlations between the two pTau217 assays and the renal function markers, including serum urea levels (*Left*) and creatinine levels (*Right*). Linear regression line with 95% CI, Spearman correlation coefficients (ρ), and P-values are shown. Aβ, amyloid-beta; BD, BD-pTau217; NT, N-terminal; Total, Total-pTau217.

Table 1. Demographic characteristics of the study cohorts

Discovery dataset	Data	CL < 10	CL = 10 to 30	CL > 30
Hong Kong Chinese discovery cohort	Sample size (*n* = 283)	137	14	132
	Amyloid-PET, CL (SD)	−2.73 (6.10)	21.47 (6.53)	73.47 (24.97)
	Plasma NULISAqpcr BD-pTau217, pg/mL (SD)	0.37 (0.65)	1.13 (2.31)	2.26 (1.90)
	Plasma Simoa pTau217, pg/mL (SD)	0.35 (0.30)	0.65 (0.61)	1.11 (0.52)
	Creatinine, μmol/L (SD)	82.13 (25.65)	78.62 (15.36)	78.97 (22.26)
	Urea, mmol/L (SD)	6.66 (2.26)	6.14 (1.58)	6.32 (2.02)
	MoCA (SD)	20.62 (6.43)	18.38 (8.10)	15.38 (5.93)
	Age, years (SD)	73.92 (7.49)	74.02 (16.05)	74.01 (7.40)
	Sex, female (%)	51.82%	57.14%	59.85%
Validation dataset	Data	CL < 10	CL = 10 to 30	CL > 30
Hong Kong Chinese validation cohort	Sample size (*n* = 146)	79	15	52
	Amyloid-PET, CL (SD)	−0.68 (4.33)	19.70 (6.29)	69.94 (23.17)
	Tau-PET global cortical-to-cerebellum [^{18}F]-T807 retention ratio (SD)	0.99 (0.04)	1.08 (0.00)	1.54 (0.16)
	Plasma NULISAqpcr BD-pTau217, pg/mL (SD)	0.21 (0.12)	1.00 (1.15)	1.96 (1.72)
	Plasma Simoa p-Tau217, pg/mL (SD)	0.27 (0.14)	0.74 (0.53)	1.23 (0.65)
	Creatinine, μmol/L (SD)	80.66 (30.94)	75.49 (18.10)	77.98 (31.97)
	Urea, mmol/L (SD)	6.03 (2.70)	5.60 (1.31)	5.99 (2.33)
	MoCA (SD)	22.15 (4.62)	19.53 (5.38)	17.81 (6.09)
	Age, years (SD)	69.70 (6.31)	73.50 (5.76)	71.31 (5.98)
	Sex, female (%)	44.30%	60.00%	76.92%

CL, Centiloid; MoCA, Montreal Cognitive Assessment; SD, SD.

exon 4a (14–16). In contrast, the Simoa ALZpath total pTau217 assay utilizes an N-terminal detector antibody that recognizes a broader spectrum of both circulating LMW and HMW tau species (Fig. 1*A*).

We first examined the correlation between plasma pTau217 concentration measured by both assays. In both the discovery and validation cohorts, BD-pTau217 and total pTau217 levels were strongly correlated (Spearman $\rho_{Discovery} = 0.89$, $p_{Discovery} = 8.31 \times 10^{-98}$; $\rho_{Validation} = 0.90$, $p_{Validation} = 6.28 \times 10^{-54}$; Fig. 1*B*), indicating that both assays reflect consistent changes in plasma pTau217 levels. Subsequently, we established a mathematical model to convert pTau217 test results between the two assays by performing Passing–Bablok regression on the combined dataset after removing outliers (*SI Appendix*, Fig. S1*A*). The regression yielded a slope of 1.37 (95% CI [CI] = 1.24 to 1.49) with an intercept of –0.11 (95% CI = –0.15 to –0.07), explaining most of the variance between assays ($R^2 = 0.90$). Nonetheless, the fitted line diverged from the identity line, and Bland–Altman analysis demonstrated proportional differences that increased with higher pTau217 levels (*SI Appendix*, Fig. S1*B*). The systematic differences in measured concentrations may arise from the distinct detection epitopes of the two assays.

Notably, individuals with chronic kidney disease exhibit elevated plasma pTau217 levels, regardless of their underlying AD pathology (3, 17, 18). This elevation may result from impaired clearance of tau species by the kidneys or dysregulation of peripherally expressed tau (18, 19). Several pTau217 assays, including the Simoa ALZpath pTau217 assay, detect both peripherally derived HMW tau and brain-derived LMW tau, making them more susceptible to systemic physiological influences. Therefore, we assessed whether an assay specifically targeting BD-pTau217 could be interfered with the kidney dysfunction. Accordingly, we performed Spearman rank correlation analysis between the plasma pTau217 levels measured by either BD-pTau217 assay or total-pTau217 assay and kidney function markers, including blood urea and creatinine. In the discovery cohort (n = 256), reduced kidney function was associated with increased total pTau217, as reflected by higher blood urea levels ($\rho = 0.12$, $P = 0.049$) and creatinine levels ($\rho = 0.18$, $P = 0.004$). In contrast, BD-pTau217 showed no association with kidney function (urea: $\rho = 0.06$, $P = 0.312$; creatinine: $\rho = 0.08$, $P = 0.197$, Fig. 1*C*).

This pattern was replicated in the independent validation cohort (n = 124), where BD-pTau217 again showed no association with kidney function (urea: $\rho = 0.02$, $P = 0.834$; creatinine: $\rho = 0.03$, $P = 0.724$). Conversely, total pTau217 exhibited a trend toward a positive association with blood urea levels ($\rho = 0.06$, $P = 0.524$; *SI Appendix*, Fig. S2) and a significant association with blood creatinine levels ($\rho = 0.16$, $P = 0.075$; *SI Appendix*, Fig. S2). Thus, these findings collectively indicate that renal impairment affects total pTau217 levels, whereas BD-pTau217 levels remain largely stable across variations in kidney function. Taken together, our results demonstrate that although total pTau217 and BD-pTau217 levels exhibited consistent changes in blood, the BD-pTau217 assay is more specific to brain-derived LMW tau species, providing a more physiologically robust signal that is less susceptible to kidney-related confounding.

Dysregulation of BD-pTau217 and Total pTau217 Levels in Individuals with Brain Aβ Pathology. Next, we assessed the dysregulations of plasma pTau217 levels measured by the BD-pTau217 and total pTau217 assays in individuals with brain Aβ pathology. In both the discovery and validation cohorts, BD-pTau217 and total pTau217 levels exhibited a stepwise upregulation in individuals with moderate (i.e., $A\beta^{Int}$) and high (i.e., $A\beta^{High}$) brain Aβ burden (Fig. 2*A*). Importantly, the median fold change (FC) of BD-pTau217 was greater than that of total pTau217 in both the $A\beta^{Int}$ group (discovery cohort: $FC_{BD\text{-}pTau217} = 2.13$, $FC_{Total\text{-}pTau217} = 1.67$; validation cohort: $FC_{BD\text{-}pTau217} = 3.40$, $FC_{Total\text{-}pTau217} = 2.31$) and $A\beta^{High}$ group (discovery cohort: $FC_{BD\text{-}pTau217} = 6.98$, $FC_{Total\text{-}pTau217} = 3.59$; validation cohort: $FC_{BD\text{-}pTau217} = 7.36$, $FC_{Total\text{-}pTau217} = 4.71$), compared to the $A\beta^{Low}$ group (Fig. 2*B*). This suggests more prominent dysregulation

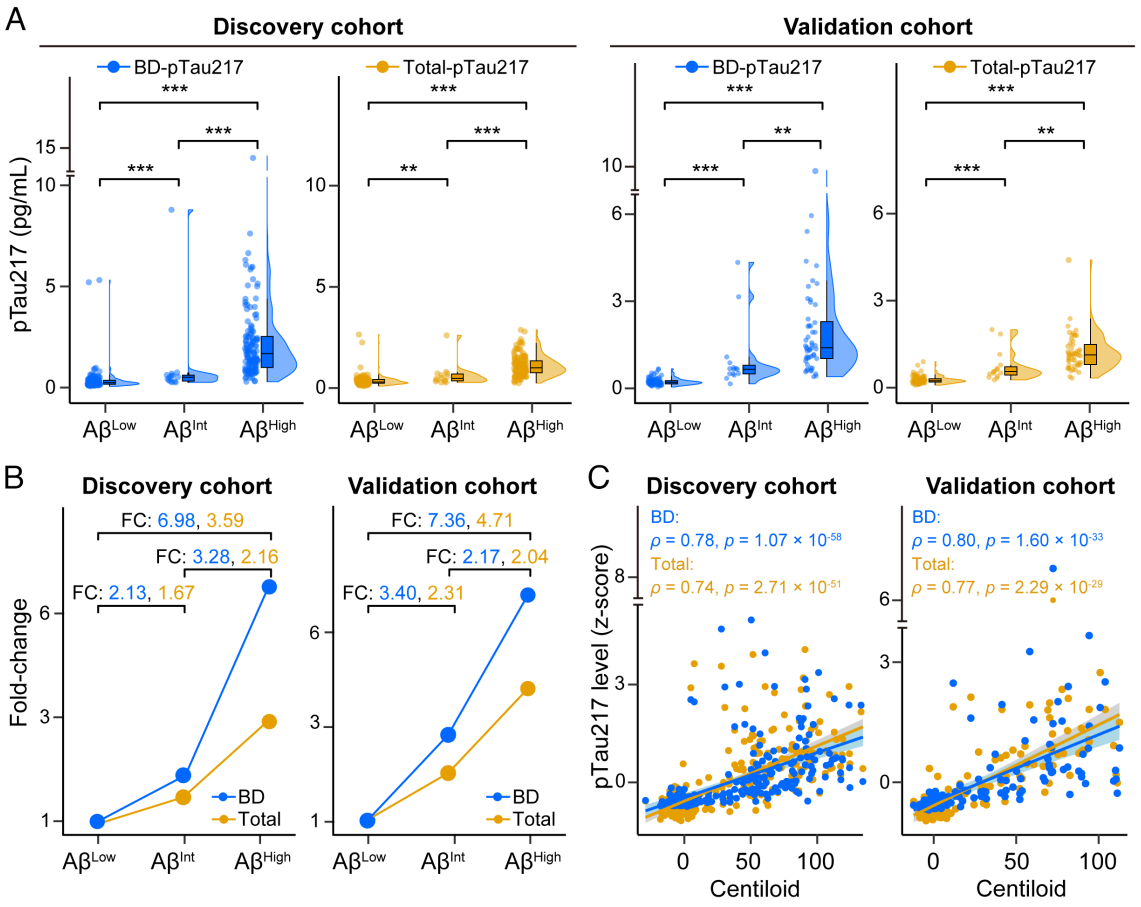

Fig. 2. Dysregulations of plasma BD-pTau217 and total-pTau217 in individuals with brain amyloid pathology. (*A*) Raincloud plots showing the distribution of plasma pTau217 levels measured by the two pTau217 assays across Aβ pathology stages in the Discovery cohort (*Left*) and Validation cohort (*Right*). Aβ stages were indexed by CL values (i.e., $A\beta^{Low}$, CL < 10; $A\beta^{Int}$, CL 10 to 30; $A\beta^{High}$, CL > 30). (*B*) Fold-changes in the median levels of plasma pTau217 measured by the two pTau217 assays across Aβ pathology stages in the Discovery cohort (*Left*) and Validation cohort (*Right*). (*C*) Scatter plots showing the correlations between the two pTau217 assays and amyloid-PET CL values in the Discovery cohort (*Left*) and Validation cohort (*Right*). For raincloud plots, the *p*-values from the Wilcoxon rank-sum test with Bonferroni adjustment are shown. For scatter plots, linear regression lines with 95% CI, Spearman correlation coefficients (ρ), and *p*-values are shown. Aβ, amyloid-beta; BD, BD-pTau217; CL, Centiloid; FC, fold-change; Total, total pTau217, $^{**}p < 0.01$, $^{***}p < 0.001$.

of BD-pTau217 upon the development of brain amyloid pathology. Association analysis between the two pTau217 assays and continuous CL values further corroborated this, with BD-pTau217 levels showing a stronger correlation with CL values ($\rho_{Discovery}$ = 0.78, $\rho_{Validation}$ = 0.80) than total pTau217 levels ($\rho_{Discovery}$ = 0.74, $\rho_{Validation}$ = 0.77) in both cohorts (Fig. 2*C*). Taken together, these results indicate that BD-pTau217 offers enhanced sensitivity and a broader dynamic range for detecting changes in brain Aβ pathology. Its stronger association with both categorical Aβ stages and continuous CL measures suggests that BD-pTau217 may serve as a more robust blood-based biomarker for indicating and staging Aβ burden compared to total pTau217.

Head-to-Head Comparison of the Performance of Plasma BD-pTau217 and Total pTau217 for Determining Brain Aβ Positivity. Plasma pTau217 has been widely studied for its diagnostic utility in classifying brain amyloid positivity (1, 3). However, the distinct associations of BD-pTau217 and total pTau217 with kidney dysfunction observed in this study suggest that differences in assay design may result in varied diagnostic performance. To evaluate this, we conducted a head-to-head comparison of the diagnostic utility of BD-pTau217 and total pTau217 for classifying Aβ pathology status in our two cohorts. In the discovery cohort, receiver operating characteristic (ROC) analyses showed that BD-pTau217 achieved higher discriminative accuracy in distinguishing $A\beta^{+}$ individuals (i.e., $A\beta^{Int}$ and $A\beta^{High}$) from $A\beta^{-}$ individuals (i.e., $A\beta^{Low}$) ($AUC_{BD\text{-}pTau217}$ = 0.96, 95% CI = 0.93 to 0.98) compared to the total pTau217 ($AUC_{Total\text{-}pTau217}$ = 0.94, 95% CI = 0.91 to 0.97; DeLong p_{diff} = 0.02; Fig. 3*A*). We observed a consistent pattern of performance improvement in the validation cohort, with BD-pTau217 achieving an AUC of 0.98 (95% CI = 0.95 to 1.00), compared to an AUC of 0.97 (95% CI = 0.95 to 0.99) for total pTau217 (DeLong p_{diff} = 0.65; Fig. 3*A*). Further evaluation of the assays' discriminative performance for Aβ–positivity, defined using previously reported CL thresholds [i.e., CL >24 or >37 as $A\beta^{+}$ (20, 21)], showed similar accuracy (*SI Appendix*, Fig. S3).

Next, we assessed the performance of the two assays across discrete Aβ stages. When distinguishing individuals with established amyloid pathology (i.e., $A\beta^{High}$) from the $A\beta^{Low}$ group, BD-pTau217 again outperformed total pTau217, achieving an AUC of 0.97 (95% CI = 0.95 to 0.99) versus 0.95 (95% CI = 0.93 to 0.98) for total pTau217 in the discovery cohort (DeLong p_{diff} = 0.02; Fig. 3*B*). Furthermore, BD-pTau217 demonstrated higher accuracy in differentiating $A\beta^{Int}$ individuals from $A\beta^{Low}$ individuals ($AUC_{BD\text{-}pTau217}$ = 0.83, 95% CI = 0.74 to 0.92) compared to total pTau217 ($AUC_{Total\text{-}pTau217}$ = 0.77, 95% CI = 0.65 to 0.89) (DeLong p_{diff} = 0.23; Fig. 3*C*), suggesting that BD-pTau217 is better at identifying early-stage amyloid pathology. Notably, BD-pTau217 also showed superior performance in distinguishing between the $A\beta^{High}$

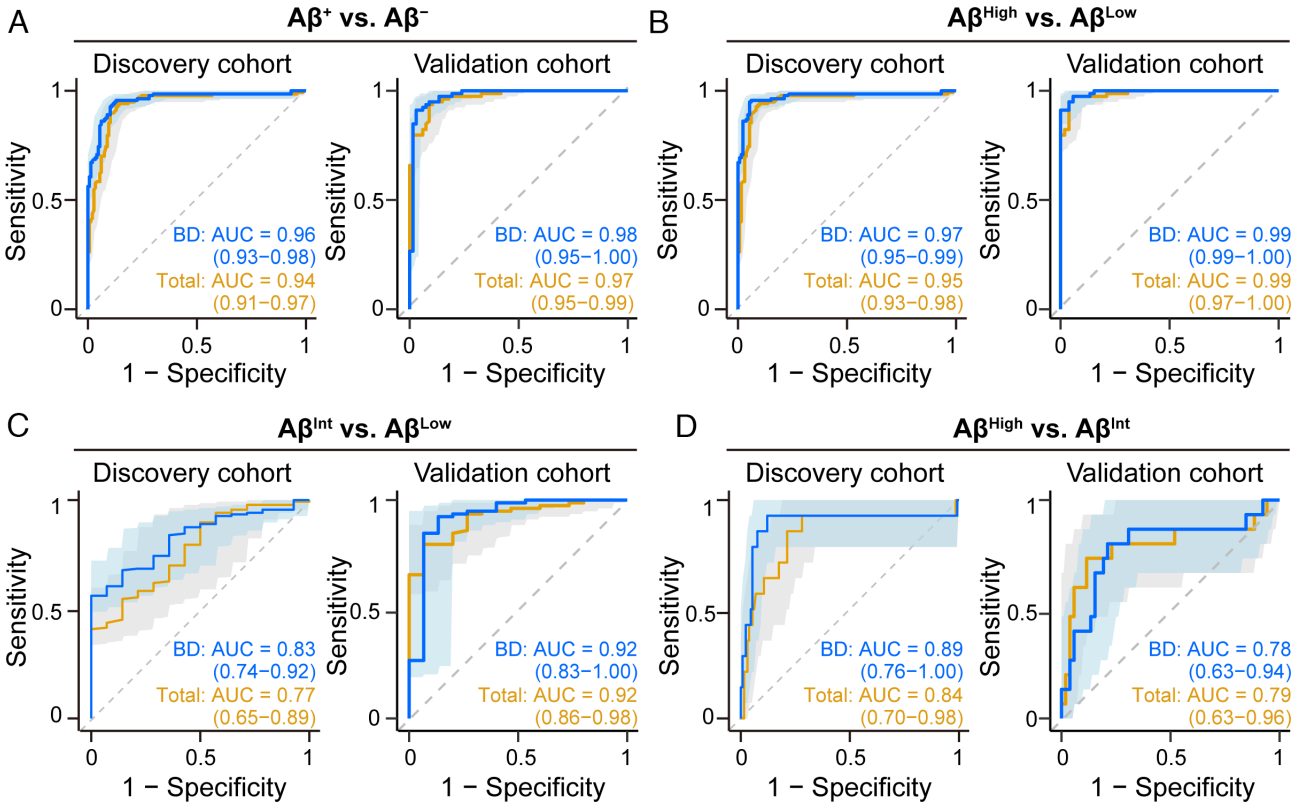

Fig. 3. Head-to-head comparison of the performance of plasma BD-pTau217 and total pTau217 assays for classifying brain Aβ pathology. (*A–D*) ROC curves with corresponding AUCs illustrating the diagnostic performance of the two pTau217 assays in classifying (*A*) $A\beta^{+}$ (i.e., CL > 10) versus $A\beta^{-}$ (i.e., CL ≤ 10) (p_{diff} = 0.02 and 0.65 in the discovery and validation cohorts, respectively), (*B*) $A\beta^{High}$ versus $A\beta^{Low}$ (p_{diff} = 0.02 and 0.19 in the discovery and validation cohorts, respectively), (*C*) $A\beta^{Int}$ versus $A\beta^{Low}$ (p_{diff} = 0.23 and 0.96 in the discovery and validation cohorts, respectively), and (*D*) $A\beta^{High}$ versus $A\beta^{Int}$ (p_{diff} = 0.01 and 0.76 in the discovery and validation cohorts, respectively). The *p*-values were calculated using DeLong's test. Aβ, amyloid-beta; AUC, area under the ROC curve; BD, BD-pTau217; CL, Centiloid; ROC, receiver operating characteristic; Total, total pTau217.

and $A\beta^{Int}$ groups ($AUC_{BD\text{-}pTau217}$ = 0.89, 95% CI = 0.76 to 1.00) compared to total pTau217 ($AUC_{Total\text{-}pTau217}$ = 0.84, 95% CI = 0.70 to 0.98; DeLong p_{diff} = 0.01; Fig. 3*D*), further corroborating its enhanced capability for staging brain amyloid pathology. Nonetheless, replication in the validation cohort did not show a significant difference between the assays in classifying different stages of brain amyloid pathology (all Delong p_{diff} > 0.05, Fig. 3 *B–D*). This lack of significant difference is likely attributable to the smaller sample size of the validation cohort, particularly after stratification into discrete Aβ stages. Overall, these results suggest that BD-pTau217 maintains excellent accuracy for differentiating Aβ pathology across disease stages. Its relatively stronger performance in differentiating borderline Aβ accumulation (i.e., $A\beta^{Int}$ versus $A\beta^{Low}$ and $A\beta^{High}$ versus $A\beta^{Int}$) highlights its potential value as a more sensitive blood-based biomarker for staging Aβ pathology.

Performance of BD-pTau217 and Total pTau217 for Staging Brain Tau Pathology. In addition to classifying amyloid pathology, several studies have reported the potential of plasma pTau217 to classify brain tau pathology, thereby enabling the staging of AD (1, 22, 23). Given that a subgroup of participants from the validation cohort underwent tau-PET examination (*n* = 128), we evaluated how the two pTau217 assays reflect tau pathology in this subgroup. The results show that both BD-pTau217 and total pTau217 levels progressively increased with rising tau pathology burden and were higher in $A\beta^{+}Tau^{+}$ (i.e., A^{+}/T^{+}) individuals compared with those who were $A\beta^{+}$ only (i.e., A^{+}/T^{-}) (Fig. 4*A*). Importantly, relative to the $A\beta^{-}Tau^{-}$ (i.e., A^{-}/T^{-}) reference group, BD-pTau217 exhibited larger fold changes than total pTau217. Specifically, compared to the A^{-}/T^{-} group, BD-pTau217 levels were 3.40-fold and 8.12-fold higher in the A^{+}/T^{-} and A^{+}/T^{+} groups, respectively (both P < 0.001), whereas total pTau217 levels were 2.67-fold and 4.79-fold higher, respectively (both P < 0.001; Fig. 4*B*).

Subsequent assessment of the performance of the two assays in identifying tau^{+} individuals showed that BD-pTau217 were more accurate ($AUC_{BD\text{-}pTau217}$ = 0.98, 95% CI = 0.96 to 0.99) than total pTau217 ($AUC_{Total\text{-}pTau217}$ = 0.95, 95% CI = 0.92 to 0.98; DeLong p_{diff} = 0.21; *SI Appendix*, Fig. S4). We further evaluated the performance of the two pTau217 assays in identifying tau positivity in $A\beta^{+}$ individuals, which is essential for staging disease progression (24). BD-pTau217 again showed higher accuracy ($AUC_{BD\text{-}pTau217}$ = 0.89, 95% CI = 0.81 to 0.97) than total pTau217 ($AUC_{Total\text{-}pTau217}$ = 0.78, 95% CI = 0.65 to 0.91 (DeLong p_{diff} = 0.49; Fig. 4*C*). Collectively, these findings indicate that compared to total pTau217, BD-pTau217 reflects brain tau pathology more sensitively and exhibits a broader dynamic response to increasing tau burden. Thus, the performance of BD-pTau217 across analyses underscores its potential as a versatile blood biomarker for monitoring both Aβ and tau pathology progression.

Establishing Reference Cutoffs of BD-pTau217 for Classifying Brain Aβ Pathology. To facilitate the clinical application of both pTau217 assays, we established cutoffs for BD-pTau217 based on the amyloid-PET data from our cohorts, comparing their performance with the well-established reference cutoffs for total pTau217 (1). Accordingly, we first evaluated binary cutoffs of BD-pTau217 and total pTau217 to determine their performance in distinguishing $A\beta^{+}$ from $A\beta^{-}$ individuals (*SI Appendix*, Fig. S5 and Table S1).

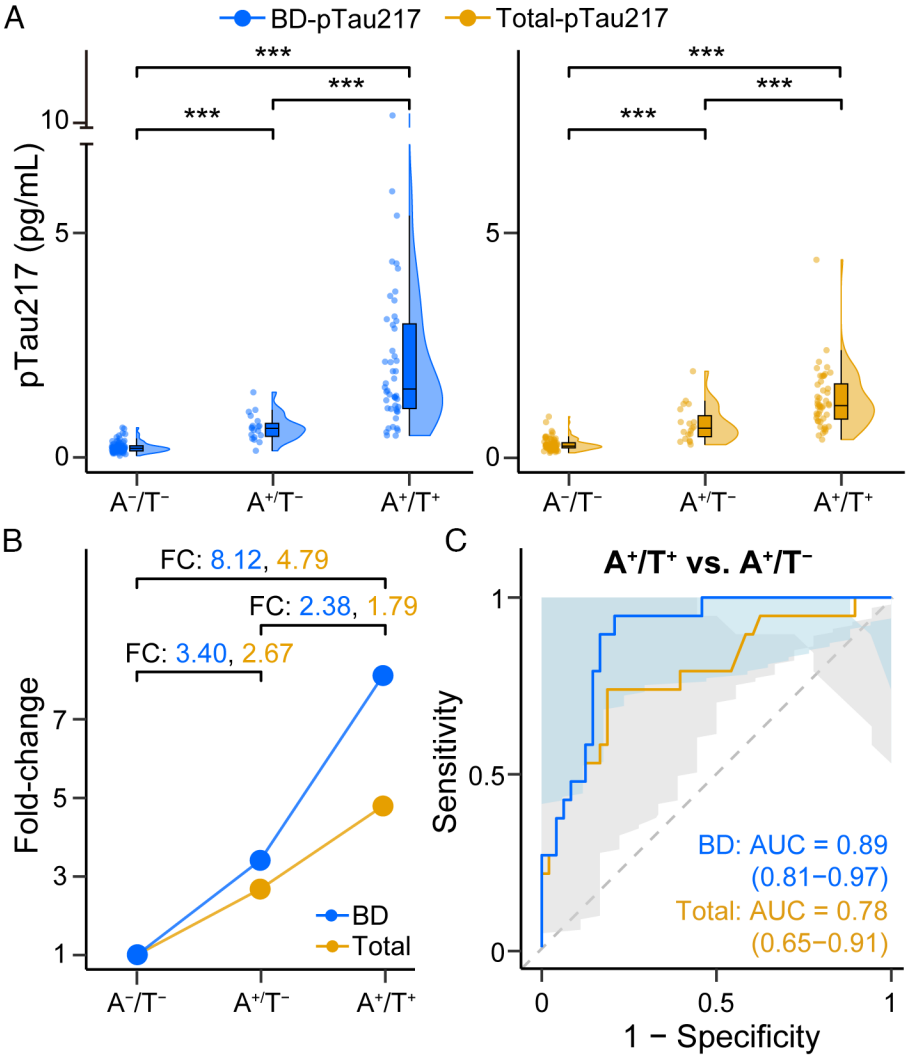

Fig. 4. Head-to-head comparison of plasma BD-pTau217 and total pTau217 assays for amyloid and tau pathology staging. (*A*) Raincloud plots showing the distribution of plasma pTau217 levels measured by the two pTau217 assays stratified by A/T positivity in a validation cohort subsample (n = 128), excluding A^-/T^+ individuals. Tau positivity was indexed by tau-PET measurements. (*B*) Fold-changes in median levels of plasma pTau217 levels measured by the two pTau217 assays across A^-/T^-, A^+/T^-, and A^+/T^+ status. (*C*) ROC curves with corresponding AUCs illustrating the diagnostic performance of the two pTau217 assays for classifying individuals in the A^+T^- versus A^+T^+ groups (p_{diff} = 0.49). For the raincloud plots, the p-values from the Wilcoxon rank-sum test with Bonferroni adjustment are shown. For the ROC curves, the p-values were calculated using DeLong's test. A, amyloid; AUC, area under the ROC curve; BD, BD-pTau217; FC, fold-change; ROC, receiver operating characteristic; T, tau; Total, total pTau217. *p < 0.05, **p < 0.01, ***p < 0.001.

For BD-pTau217, the optimal binary cutoff of >0.66 pg/mL was derived using the Youden index in the discovery cohort, yielding 86.99% sensitivity, 95.62% specificity, and 91.17% overall percent agreement (OPA) in the discovery cohort. In the validation cohort, this cutoff demonstrated 74.63% sensitivity, 100% specificity, and 88.36% OPA (*SI Appendix*, Table S1). This performance is slightly superior to that of the total pTau217 binary cutoff (i.e., >0.42 pg/mL) (1), which has 90.41 to 91.04% sensitivity, ranging from 79.56% to 89.87% specificity, and an OPA of 85.16 to 90.40%.

Given that a three-range cutoff strategy is increasingly being adopted to enhance diagnostic performance in clinical settings (1, 25, 26), we defined the lower and upper reference points of BD-pTau217 to correspond to thresholds that yield 95% sensitivity and 95% specificity in the discovery cohort. Based on this strategy, individuals with a BD-pTau217 level above the upper cutoff (>0.66 pg/mL) or below the lower cutoff (<0.36 pg/mL) will be classified as having a positive or negative signal, respectively (*SI Appendix*, Fig. S6). Individuals with a BD-pTau217 level between the upper and lower cutoff points will be classified into an intermediate group and referred for confirmatory testing, such as cerebrospinal fluid biomarker assessment or amyloid-PET imaging (25, 26).

Applying this three-range cutoff strategy showed that BD-pTau217 achieved highly accurate classification of brain amyloid pathology with an OPA of 94.63 to 98.39% across cohorts, surpassing total pTau217, which used two cutoffs (i.e., lower and upper cutoffs: <0.40 and >0.63 pg/mL) with an OPA of 92.67 to 93.75% (Table 2). Moreover, this three-range cutoff strategy of BD-pTau217 achieved 95.21 to 97.01% sensitivity, 95.62 to 100% specificity, 95.49 to 100% positive predictive value (PPV), and 93.58 to 97.30% negative predictive value (NPV) across both cohorts, outperforming total pTau217 (91.04 to 91.10% sensitivity, 97.08 to 97.47% specificity, 96.30 to 96.55% PPV, and 88.79 to 91.89% NPV). Importantly, both pTau217 assays meet the recently published acceptable performance of an AD blood test with two cutoffs for clinical use (27), classifying less than 20% of individuals into the intermediate group: BD-pTau217 classified 14.49 to 15.07%, while total pTau217 classified 12.33 to 18.02% of individuals as intermediate (i.e., 0.36 to 0.66 and 0.40 to 0.63 pg/mL, respectively). Thus, by establishing a three-range cutoff strategy in our amyloid-PET–characterized cohorts, we demonstrated the high performance of BD-pTau217 in assessing brain Aβ pathology. This approach ensures high accuracy, a manageable percentage of individuals classified as intermediate, and excellent reproducibility across cohorts. These characteristics highlight the practical utility of BD-pTau217 for clinical triage and integration into diagnostic workflows.

Discussion

While pTau217 is increasingly being studied as a promising biomarker for facilitating the diagnosis of AD, the presence of peripheral sources of tau and pTau217 can potentially interfere with test

Table 2. Three-range reference of plasma BD-pTau217 and total pTau217 for classifying brain amyloid positivity

Three-range reference for Aβ positivity: Plasma BD-pTau217 positive: >0.66 pg/mL Plasma BD-pTau217 negative: <0.36 pg/mL			Three-range reference for Aβ positivity: Plasma total-pTau217 positive: >0.63 pg/mL Plasma total-pTau217 negative: <0.40 pg/mL		
Characteristic	Discovery	Validation	Characteristic	Discovery	Validation
n	283	146	*n*	283	146
Aβ-positive, *n* (%)	146 (51.59%)	67 (45.89%)	Aβ-positive, *n* (%)	146 (51.59%)	67 (45.89%)
Plasma BD-pTau217 positive, *n* (%)	133 (47.00%)	50 (34.25%)	Plasma total-pTau217 positive, *n* (%)	116 (40.99%)	54 (36.99%)
Plasma BD-pTau217 intermediate group, *n* (%)	41 (14.49%)	22 (15.07%)	Plasma total-pTau217 intermediate group, *n* (%)	51 (18.02%)	18 (12.33%)
Plasma BD-pTau217 negative, *n* (%)	109 (38.52%)	74 (50.68%)	Plasma total-pTau217 negative, *n* (%)	116 (40.99%)	74 (50.68%)
Sensitivity of lower reference point, %	95.21%	97.01%	Sensitivity of lower reference point, %	91.10%	91.04%
Specificity of upper reference point, %	95.62%	100.00%	Specificity of upper reference point, %	97.08%	97.47%
PPV, upper reference point, %	95.49%	100.00%	PPV, upper reference point, %	96.55%	96.30%
NPV, lower reference point, %	93.58%	97.30%	NPV, lower reference point, %	88.79%	91.89%
OPA for BD-pTau217 positive and negative, %	94.63%	98.39%	OPA for total-pTau217 positive and negative, %	92.67%	93.75%

Aβ, amyloid-beta; NPV, negative predictive value; OPA, overall percent agreement; PPV, positive predictive value.

results, leading to increased false-positive or false-negative cases, thereby reducing diagnostic accuracy. Therefore, a blood-based assay that specifically targets the brain-derived form of pTau217 could provide a solution for highly specific detection of AD-related brain pathology. In this study, we conducted a head-to-head comparison of BD-pTau217 and total pTau217, evaluating their ability to classify brain amyloid and tau pathology. Our results demonstrate that, compared to total pTau217, BD-pTau217 is less affected by kidney dysfunction and exhibits a stronger association with amyloid-PET Centiloid than total pTau217. BD-pTau217 also provides superior sensitivity and specificity in detecting individuals with Aβ pathology. Furthermore, BD-pTau217 outperforms total pTau217 in distinguishing between different stages of tau pathology, enabling more accurate disease staging. Collectively, these findings highlight the potential of BD-pTau217 as a highly specific and sensitive blood-based biomarker for early classification and staging of AD.

It is important to recognize that total Tau protein is not exclusively expressed in the brain, but is also present in various human tissues and organs, including the pancreas, kidneys, and peripheral nerves (9, 15, 28). Consequently, pathological changes in these organs—such as neurodegeneration outside the CNS or kidney dysfunction—can result in elevated plasma pTau217 levels independently of AD-related brain pathology. For example, individuals with chronic kidney diseases exhibit elevated plasma pTau217 levels (12, 17), which are positively associated with markers of kidney dysfunction, including a decreased estimated glomerular filtration rate (eGFR) (17, 29). Peripheral neuronal damage, as observed in ALS, can also result in increased blood pTau217 levels (6, 15). As a result, assays that measure peripheral or total pTau may perform poorly in distinguishing peripheral changes from brain-specific pathological changes. Consistent with this concept, our study showed that total pTau217 assay results are positively associated with blood levels of creatinine and urea, both established markers of kidney dysfunction, regardless of brain amyloid status. Moreover, we observed that 2.34%-5.48% of $A\beta^-$ individuals were misclassified as $A\beta^+$ when using total pTau217, likely because of the positive bias introduced by impaired kidney function, which elevates total pTau217 levels in $A\beta^-$ individuals. In contrast, the BD-pTau217 assay, which specifically recognizes brain-derived LMW tau isoform (lacking exon 4a), was not associated with markers of kidney dysfunction and significantly reduced the false-positive rate among $A\beta^-$ individuals to 0 to 2.12%. Furthermore, the BD-pTau217 assay demonstrated greater sensitivity for detecting early amyloid pathological changes, as evidenced by a larger fold-change (FC = 2.13 to 3.40) in individuals with Centiloid values from 10 to 30, compared to the total pTau217 assay (FC = 1.67 to 2.31). Taken together, these findings demonstrate that an assay targeting brain-specific tau splicing isoforms can effectively eliminate interference from peripheral changes and dysfunctions, potentially leading to highly sensitive and specific detection of AD-related pathological changes in the brain.

Recent clinical practice guidelines on the use of blood-based biomarkers for AD diagnosis recommend that a blood test should achieve ≥90% sensitivity and specificity to serve as a substitute for amyloid PET imaging or cerebrospinal fluid AD biomarker testing in patients with cognitive impairment, specifically for confirming brain amyloid pathology (30). In the present study, by employing a three-range cutoff strategy (i.e., negative < 0.36 pg/mL, intermediate 0.36 to 0.66 pg/mL, and positive > 0.66 pg/mL), we demonstrated that BD-pTau217 achieves 95.21 to 97.01% sensitivity, 95.62 to 100% specificity, 93.58 to 97.30% NPV, and 95.49 to 100% PPV for the classification of brain amyloid positivity, making it superior to total pTau217. These results suggest that the BD-pTau217 assay has strong potential to be implemented as a high-performance diagnostic tool for detecting brain amyloid pathology in clinical settings. Furthermore, as suggested by recent AD diagnostic criteria, the classification of tau-related pathological changes can provide critical evidence for biological disease staging (24). Importantly, our study shows that BD-pTau217 performs better than total pTau217 in differentiating $A\beta^+Tau^+$ and $A\beta^+Tau^-$ individuals (AUC = 0.89 versus 0.78, respectively). Thus, this capacity to accurately distinguish tau pathology stages highlights the potential of BD-pTau217 for the detection of brain amyloid positivity as well as the precise staging of AD, which is critical for disease prognosis and monitoring. Nonetheless, effective treatment and management of AD require a comprehensive assessment of disease status that goes beyond amyloid- and tau-related changes, encompassing diverse biological

processes such as neuronal, immune, vascular, and metabolic pathways (31–36). Therefore, the future integration of BD-pTau217 with biomarkers that reflect these additional pathways may be the optimal strategy for the clinical implementation of AD blood biomarker assays. Such a multimarker approach would enable a more accurate and holistic overview of disease status and prognosis, which are key elements for optimizing therapeutic strategies and improving patient outcomes.

In the current study, we compared two pTau217 assays implemented on different proteomic platforms: NULISAqpcr and Simoa. These platforms utilize distinct calibrators and quantification methods, making it challenging to directly compare the absolute levels of BD-pTau217 and total pTau217 proteins. Nevertheless, pilot studies have indicated that only approximately one-fifth of total tau protein in plasma originates from the brain (14, 37), highlighting the necessity of ultrasensitive detection platforms for accurate measurement of BD-pTau217. To date, two proteomic platforms have demonstrated strong capabilities for quantifying BD-pTau217: Lilly's pTau217 electrochemiluminescence immunoassay on the Meso Scale Discovery (MSD) platform and Alamar Biosciences's NULISAqpcr platform, which is based on an improved proximity extension assay. The Lilly MSD assay has been extensively validated across diverse cohorts, consistently shows high concordance with brain amyloid pathology and outperforms the Simoa ALZpath pTau217 assay for differentiating ALS from AD (15, 38). In our study, we further demonstrated that the NULISAqpcr-based BD-pTau217 assay is less affected by kidney dysfunction and provides superior performance in classifying brain amyloid and tau pathologies compared to the Simoa assay. Therefore, both ultrasensitive platforms hold significant promise for enabling the clinical application of BD-pTau217 assays. Future head-to-head comparisons and cross-validation studies between these two BD-pTau217 assays will be crucial to further establish their utility and reliability in clinical settings. Additionally, it would be valuable to investigate whether enhanced chemiluminescence immunoassays (CLIA) can accurately measure BD-pTau217, because this approach may facilitate the large-scale implementation of this assay in population health screening and routine clinical diagnostics.

This study has several limitations that should be acknowledged. First, all participants in our two cohorts were of Chinese ethnicity, which raises uncertainty about whether the BD-pTau217 assay exhibits similarly high performance in populations of other ethnic backgrounds. Recent studies suggest that race and ethnicity can significantly influence the levels of AD-related blood biomarkers, including pTau (39). Therefore, future validation of this assay in diverse ethnic groups is essential to confirm its generalizability. Second, in the current study, we assessed the performance of two pTau217 assays for classifying overall brain amyloid and tau pathologies. It would be valuable to investigate whether BD-pTau217 also demonstrates stronger associations with amyloid- or tau-related pathological changes in specific brain regions. Such analyses could further support the assay's specificity for AD and provide deeper insights into its biological relevance in disease pathogenesis. Third, although we showed that BD-pTau217 is strongly correlated with brain amyloid-PET Centiloid data, the specificity of this assay for AD-related pathological changes requires further validation in cohorts that include patients with other neurological or neurodegenerative disorders. Expanding the scope of evaluation will help establish the robustness and clinical utility of BD-pTau217 as a diagnostic biomarker.

In conclusion, our head-to-head comparison between BD-pTau217 and total pTau217 assays demonstrates that BD-pTau217 is less affected by peripheral changes, such as kidney dysfunction, and offers superior specificity and sensitivity for the classification and staging of AD-related brain pathology. These findings pave the way for the development of highly specific and sensitive blood-based diagnostic tools for AD that have significant potential to enhance early detection, disease staging, and patient management in clinical settings.

Materials and Methods

Participant Recruitment. We recruited 429 participants from the Hong Kong Chinese population. The cohort comprised individuals aged 32 y or older who visited the specialist outpatient clinics of the Department of Medicine and Therapeutics at the Prince of Wales Hospital, Department of Medicine at Queen Mary Hospital, Department of Medicine and Geriatrics at Tuen Mun Hospital, Department of Medicine and Geriatrics at United Christian Hospital, Department of Medicine & Geriatrics at Ruttonjee & Tang Shiu Kin Hospitals, and Department of Medicine at Queen Elizabeth Hospital. Participants underwent clinical examination, the Montreal Cognitive Assessment (MoCA) (40), blood collection for the measurement of biomarkers, amyloid-PET using [^{11}C]-Pittsburgh Compound B (PiB), tau-PET using ^{18}F-Flortaucipir (T807), and neuroimaging by MRI (41). Each participant's age and sex were recorded.

This study was approved by the Joint Chinese University of Hong Kong–New Territories East Cluster Clinical Research Ethics Committee at CUHK-PWH (CREC ref. No. 2015.461), the Institutional Review Board, Hospital Authority (UW 22-027, CIRB-2023-065-1, KC/KE-22-0107/ER-2, and KC/KE-15-0024/FR-3), and the Human and Artefacts Research Ethics Committee (HAREC) at HKUST (CRP#180, CRP#225, HREP-2023-0179). All participants or the legal guardians of participants with advanced dementia provided written informed consent for study participation and sample collection.

Imaging Acquisition and Quantification. T1-weighted structural images were acquired using 3-T MRI scanners. Amyloid-PET imaging was performed using ^{11}C-PiB PET (detailed in *SI Appendix*, Figs. S7–S9, Tables S2 and S3, and *Supplementary Methods* S1 and S2). All participants were assigned to the $A\beta^{Low}$, $A\beta^{Int}$, or $A\beta^{High}$ group according to their amyloid status on PET, irrespective of their cognitive status. Low, intermediate, and high Aβ pathology on Aβ-PET were defined as <10, 10 to 30, and >30 CL units, respectively. Tau-PET imaging was performed using ^{18}F-T807 (n = 146). The data were acquired from 85 to 95 min postinjection at Hong Kong Sanatorium & Hospital. The Tau burden was calculated semiquantitatively by qualified radiologists and the global cortical-to-cerebellum SUV ratio ≧ 1.14 was used as the cut-off for abnormality in Tau burden (*SI Appendix*, Table S4).

Plasma BD-pTau217 Measurement. We measured plasma BD-pTau217 levels on an Alamar ARGO HT system using the commercially available NULISAqpcr BD-pTau217 Assay (Cat. No. 801430, Alamar Biosciences). Briefly, we centrifuged thawed plasma at 10,000× g for 10 min to remove particulates. We analyzed 35 µL plasma following the manufacturer's instructions and quantified BD-pTau217 levels by real-time PCR (qPCR). The assay has a quantification range from 0.09 to 1,355.90 pg/mL. The kit contains quality controls with high (C1, functional value: 293.55 pg/mL) or low (C2, functional value: 3.31 pg/mL) assigned pTau217 concentrations. The interassay coefficients of variation for C1 and C2 were 2.4% and 16.51%, respectively. We retested samples if an error was reported and repeated the experiment if the quality control sample measured was outside the range specified on the certificate of analysis or if the calibration curve was poorly fitted.

Plasma Total pTau217 Measurement. We measured plasma total pTau217 levels on a Quanterix HD-X using the commercially available Simoa ALZpath p-Tau 217 Advantage PLUS Reagent Kit (Cat. No. 104570, Quanterix). Briefly, on the day of analysis, we brought the plasma samples to room temperature and centrifuged them at 10,000× g for 5 min to remove particulates. Threefold, on-board sample dilution was performed automatically on the instrument. We prepared the control samples and reagents according to the manufacturer's instructions. We measured samples in duplicate and report the mean concentrations herein. This assay has a quantification range from 0.00244 to 10.0 pg/mL. The kit contains quality controls with low (QC1, mean concentration: 0.758 pg/mL) or high (QC2, mean concentration: 8.28 pg/mL) assigned pTau217 concentrations. The interassay coefficients of variation for QC1 and QC2 were 5.3% and 7.7%, respectively. We retested samples if an error was reported or the replicate coefficient of variation was greater than 20%. We repeated the experiment if the quality control sample

measured was outside the range specified on the certificate of analysis or if the calibration curve was poorly fitted.

Statistical Analysis and Data Visualization. We performed most statistical analyses and figure generation using R (version 4.4.2). For cohort characterization, we used the Wilcoxon rank-sum test with Bonferroni adjustment to compare continuous variables between groups. We applied Spearman's rank correlation to evaluate the strength and direction of associations between continuous variables. We fitted Passing–Bablok regression for agreement assessment using custom-written Python code. We conducted Bland–Altman analysis using the built-in function in Prism (version 10.6.0). We assessed discriminative performance using ROC analysis and generated ROC curves with the *ggroc()* function in the pROC package (v1.18.5) (42). We evaluated statistical differences between ROC curves using DeLong's test. We determined optimal cutoffs using the Youden index with the *coords()* function in the pROC package. The level of statistical significance for all comparisons was set at $p < 0.05$, and 95% CI were calculated. We generated all plots using the *ggplot()* function in the ggplot2 package (v3.5.1) (43).

Data, Materials, and Software Availability. All other data are available from the corresponding author upon reasonable request. The consent forms signed by participants state that the research content will be kept private under the supervision of the hospital and research team. Therefore, the phenotypic and proteomic data of participants will only be available and shared in formal collaborations. A review panel hosted at HKUST will process and review any applications for data sharing and project collaboration and promptly notify applicants of the decision. Researchers may contact HKUST (sklneurosci@ust.hk) for details about data sharing and project collaboration related to the present study. The codes for our statistical analyses and data visualization are publicly available at: https://github.com/yjiangah/BDpTau217_study/ (44). All statistical data associated with this study are contained in the main text or *SI Appendix*.

ACKNOWLEDGMENTS. We express our sincerest gratitude to the participants of the Hong Kong Chinese cohort, along with their relatives at the Prince of Wales Hospital of the Chinese University of Hong Kong (CUHK-PWH), Queen Mary Hospital (QMH), United Christian Hospital (UCH), Tuen Mun Hospital (TMH), Ruttonjee & Tang Shiu Kin Hospitals (RTSKH), and Queen Elizabeth Hospital (QEH), without whom this research would not have been possible. We also thank Dr. Bonnie W.Y. Wong, Mr. Ronnie M.N. Lo, Mrs. Elaine Y.L. Cheng, Dr. Patrick Ka Chun Chiu (QMH), Dr. Ka Keung Yam (QMH), Dr. Edmond Kwok Yiu Sha (UCH), Dr. Ting Kwan Yim (UCH), Dr. Sze Yuen Fung (UCH), Dr. Ping Cheong Ho (UCH), Dr. Kathy Ka Ling Wong (UCH), Dr. Iki Hoi Ki Chan (UCH), Yuen Yee Tam (UCH), Mei Ling Lau (UCH), Dr. Wai Ming Wong (TMH), Dr. Tung Yi Fu (TMH), Dr. Hiu Ki Yam (TMH), Chung Ho Chan (TMH), Dr. Carolyn Poey Lyn KNG (RTSKH), Dr. WONG Chit Wai (RTSKH), Dr. KWAN Chung Hon, Noble (RTSKH), Dr. WONG Che Keung (RTSKH), and Mr. CHAN Tak Sing (RTSKH), and Choi Siu Man (QEH) for coordinating the collection of clinical samples and data. Y.J. is a recipient of the Hong Kong Postdoctoral Fellowship Award from the Research Grants Council of the Hong Kong Special Administrative Region, China (Project No. HKUST PDFS2324-6S04). H.Z. is a Wallenberg Scholar and a Distinguished Professor at the Swedish Research Council supported by grants from the Swedish Research Council (#2023-00356, #2022-01018, and #2019-02397), the European Union's Horizon Europe Research and Innovation Programme under grant agreement No. 101053962, Swedish State Support for Clinical Research (#ALFGBG-71320), the Alzheimer Drug Discovery Foundation (ADDF), USA (#201809-2016862), the AD Strategic Fund and the Alzheimer's Association (#ADSF-21-831376-C, #ADSF-21-831381-C, #ADSF-21-831377-C, and #ADSF-24-1284328-C), the European Partnership on Metrology co-financed by the European Union's Horizon Europe Research and Innovation Programme and the Participating States (NEuroBioStand, #22HLT07), the Bluefield Project, Cure Alzheimer's Fund, the Olav Thon Foundation, the Erling-Persson Family Foundation, Familjen Rönströms Stiftelse, Familjen Beiglers Stiftelse, Stiftelsen för Gamla Tjänarinnor, Hjärnfonden, Sweden (#FO2022-0270), the European Union's Horizon 2020 Research and Innovation Programme under the Marie Skłodowska-Curie grant agreement No. 860197 (MIRIADE), the European Union Joint Programme – Neurodegenerative Disease Research (JPND2021-00694), the NIH and Care Research University College London Hospitals Biomedical Research Centre, the UK Dementia Research Institute at UCL (UKDRI-1003), and an anonymous donor. This study was supported in part by the Research Grants Council of Hong Kong (the Theme-Based Research Scheme [T13-605/18 W] and the General Research Fund [HKUST16104624 and HKUST16102824]), the Areas of Excellence Scheme of the University Grants Committee (AoE/M-604/16), the InnoHK initiative of the Innovation and Technology Commission of the Hong Kong Special Administrative Region Government, the Innovation and Technology Fund for State Key Laboratory (ITCPD/17-9), the SIAT–HKUST Joint Laboratory for Brain Science (Joint Laboratory Funding Scheme [JLFS/M-604/24]), and the Guangdong–Hong Kong Joint Laboratory for Psychiatric Disorders (2023B1212120004).

Author affiliations: [a]Division of Life Science, State Key Laboratory of Nervous System Disorders and Daniel and Mayce Yu Molecular Neuroscience Center, The Hong Kong University of Science and Technology, Hong Kong Special Administrative Region, China; [b]InnoHK Hong Kong Center for Neurodegenerative Diseases, Hong Kong Special Administrative Region, China; [c]Guangdong Provincial Key Laboratory of Brain Science, Disease and Drug Development, Hong Kong University of Science and Technology Shenzhen Research Institute, Shenzhen-Hong Kong Institute of Brain Science, Shenzhen, Guangdong 518057, China; [d]Department of Medicine, Queen Elizabeth Hospital, Hospital Authority, Hong Kong Special Administrative Region, China; [e]Department of Medicine and Geriatrics Ruttonjee & Tang Shiu Kin Hospitals, Hong Kong Special Administrative Region, China; [f]Department of Medicine and Geriatrics, Tuen Mun Hospital, New Territories West Cluster, Hospital Authority, Tuen Mun, Hong Kong Special Administrative Region, China; [g]Division of Geriatrics, Department of Medicine, School of Clinical Medicine, The University of Hong Kong, Pokfulam, Hong Kong Special Administrative Region, China; [h]Department of Medicine and Geriatrics, United Christian Hospital, Hospital Authority, Kwun Tong, Hong Kong Special Administrative Region, China; [i]Division of Neurology, Department of Medicine and Therapeutics, Lau Tat-chuen Research Centre of Brain Degenerative Diseases in Chinese, Gerald Choa Neuroscience Institute, Lui Che Woo Institute of Innovative Medicine, Li Ka Shing Institute of Health Sciences, The Chinese University of Hong Kong, Shatin, Hong Kong Special Administrative Region, China; [j]Division of Geriatrics, Department of Medicine and Therapeutics, Therese Pei Fong Chow Research Centre for Prevention of Dementia, The Chinese University of Hong Kong, Shatin, Hong Kong Special Administrative Region, China; [k]Department of Neurodegenerative Disease, Queen Square Institute of Neurology, University College London, London WC1N 3BG, United Kingdom; [l]United Kingdom Dementia Research Institute, University College London, London NW1 3BT, United Kingdom; [m]Department of Psychiatry and Neurochemistry, Institute of Neuroscience and Physiology, the Sahlgrenska Academy at the University of Gothenburg, Mölndal, Göteborg 13 46, Sweden; [n]Clinical Neurochemistry Laboratory, Sahlgrenska University Hospital, Mölndal SE-43180, Sweden; [o]Wisconsin Alzheimer's Disease Research Center, University of Wisconsin School of Medicine and Public Health, University of Wisconsin-Madison, Madison, WI 53792-2420; [p]Department of Pathology and Laboratory Medicine, University of Wisconsin School of Medicine and Public Health, Madison, WI 53705; [q]Centre for Brain Research, Indian Institute of Science, Bangalore 560012, India; and [r]Shenzhen Institutes of Advanced Technology-Hong Kong University of Science and Technology Joint Laboratory for Brain Science, Shenzhen, Guangdong 518055, China

Author contributions: Y.J., A.K.Y.F., and N.Y.I. designed research; Y.J., W.Z., and L.K.W.C. performed experiments; Y.J., W.Z., and Z.X. contributed new analytic tools; Y.J., W.Z., Z.X., W.W.W., L.K.W.C., K.Y.M., H.Y.W., H.Z., A.K.Y.F., and N.Y.I. analyzed data; F.C.I., S.M.C., A.L.T.C., C.Y.L., K.S.H., C.K.S., J.K.Y.Y., Y.F.S., H.M.W., V.C.T.M., T.C.Y.K., and H.M.W. organized patient recruitment and sample collection; and Y.J., W.Z., Z.X., A.K.Y.F., and N.Y.I. wrote the paper.

Reviewers: S.G., Icahn School of Medicine at Mount Sinai; and V.M.L., University of Pennsylvania Department of Pathology and Laboratory Medicine.

Competing interest statement: Y.J., F.C.I., A.K.Y.F., and N.Y.I. are inventors of related technology licensed to Cognitact. Y.J. and F.C.I. are co-founders of Cognitact. H.Y.W. is consultant for Cognitact. H.Z. has served on scientific advisory boards and/or as a consultant for AbbVie, Acumen, Alector, Alzinova, ALZpath, Amylyx, Annexon, Apellis, Artery Therapeutics, AZTherapies, Cognito Therapeutics, CogRx, Denali, Eisai, Enigma, LabCorp, Merck Sharp & Dohme, Merry Life, Nervgen, Novo Nordisk, Optoceutics, Passage Bio, Pinteon Therapeutics, Prothena, Quanterix, Red Abbey Labs, reMYND, Roche, Samumed, ScandiBio Therapeutics AB, Siemens Healthineers, Triplet Therapeutics, and Wave; has given lectures sponsored by Alzecure, BioArctic, Biogen, Cellectricon, Fujirebio, LabCorp, Lilly, Novo Nordisk, Oy Medix Biochemica AB, Roche, and WebMD; is a co-founder of Brain Biomarker Solutions in Gothenburg AB (BBS), which is a part of the GU Ventures Incubator Program; and is a shareholder of MicThera (outside submitted work). All other authors declare no conflicts of interest.

1. N. J. Ashton *et al.*, Diagnostic accuracy of a plasma phosphorylated tau 217 immunoassay for Alzheimer disease pathology. *JAMA Neurol.* **81**, 255–263 (2024).
2. S. Palmqvist *et al.*, Blood biomarkers to detect Alzheimer disease in primary care and secondary care. *JAMA* **332**, 1245–1257 (2024).
3. S. Palmqvist *et al.*, Plasma phospho-tau217 for Alzheimer's disease diagnosis in primary and secondary care using a fully automated platform. *Nat. Med.* **31**, 2036–2043 (2025).
4. G. Lan *et al.*, Comprehensive evaluation of plasma tau biomarkers for detecting and monitoring Alzheimer's disease in a multicenter and multiethnic aging population. *Nat. Aging* **5**, 1601–1618 (2025).
5. N. Warmenhoven *et al.*, A comprehensive head-to-head comparison of key plasma phosphorylated tau 217 biomarker tests. *Brain* **148**, 416–431 (2025).
6. S. Abu-Rumeileh *et al.*, Phosphorylated tau 181 and 217 are elevated in serum and muscle of patients with amyotrophic lateral sclerosis. *Nat. Commun.* **16**, 2019 (2025).

7. K. A. Q. Cousins *et al.*, Elevated plasma phosphorylated tau 181 in amyotrophic lateral sclerosis. *Ann. Neurol.* **92**, 807–818 (2022).
8. S. Janelidze *et al.*, A comparison of p-tau assays for the specificity to detect tau changes in Alzheimer's disease. *Alzheimer's Dement.* **21**, e70208 (2025).
9. S. Buchholz, H. Zempel, The six brain-specific tau isoforms and their role in Alzheimer's disease and related neurodegenerative dementia syndromes. *Alzheimers Dement.* **20**, 3606–3628 (2024).
10. I. Fischer, P. W. Baas, Resurrecting the mysteries of big tau. *Trends Neurosci.* **43**, 493–504 (2020).
11. C. Groot *et al.*, Diagnostic and prognostic performance to detect Alzheimer's disease and clinical progression of a novel assay for plasma p-tau217. *Alzheimers Res. Therapy* **14**, 67 (2022).
12. M. M. Mielke *et al.*, Performance of plasma phosphorylated tau 181 and 217 in the community. *Nat. Med.* **28**, 1398–1405 (2022).
13. F. Gonzalez-Ortiz *et al.*, Plasma brain-derived tau is an amyloid-associated neurodegeneration biomarker in Alzheimer's disease. *Nat. Commun.* **15**, 2908 (2024).
14. F. Gonzalez-Ortiz *et al.*, Brain-derived tau: A novel blood-based biomarker for Alzheimer's disease-type neurodegeneration. *Brain* **146**, 1152–1165 (2023).
15. S. Janelidze *et al.*, A comparison of p-tau assays for the specificity to detect tau changes in Alzheimer's disease. *Alzheimers Dement.* **21**, e70208 (2025).
16. D. Bali *et al.*, Comparison of plasma ALZpath p-Tau217 with Lilly p-Tau217 and p-Tau181. *Alzheimers Dement.* **20**, e088984 (2024).
17. J. A. Bornhorst *et al.*, Quantitative assessment of the effect of chronic kidney disease on plasma P-Tau217 concentrations. *Neurology* **104**, e210287 (2025).
18. F. Gasparini *et al.*, Kidney function, Alzheimer disease blood biomarkers, and dementia risk in community-dwelling older adults. *Neurology* **106**, e214446 (2026).
19. J. Wang *et al.*, Physiological clearance of tau in the periphery and its therapeutic potential for tauopathies. *Acta Neuropathol.* **136**, 525–536 (2018).
20. M. A. Mintun *et al.*, Donanemab in early Alzheimer's disease. *N. Engl. J. Med.* **384**, 1691–1704 (2021).
21. J. R. Sims *et al.*, Donanemab in early symptomatic Alzheimer disease: The TRAILBLAZER-ALZ 2 randomized clinical trial. *JAMA* **330**, 512–527 (2023).
22. A. Feizpour *et al.*, Detection and staging of Alzheimer's disease by plasma pTau217 on a high throughput immunoassay platform. *eBioMedicine* **109**, 105405 (2024).
23. D. Shin *et al.*, Potential utility of plasma pTau217 for assessing amyloid and tau biomarker profiles. *Eur. J. Nucl. Med. Mol. Imaging* **53**, 518–530 (2025).
24. C. R. Jack Jr. *et al.*, Revised criteria for diagnosis and staging of Alzheimer's disease: Alzheimer's Association workgroup. *Alzheimers Dement.* **20**, 5143–5169 (2024).
25. O. Hansson *et al.*, The Alzheimer's association appropriate use recommendations for blood biomarkers in Alzheimer's disease. *Alzheimers Dement.* **18**, 2669–2686 (2022).
26. W. S. Brum *et al.*, A two-step workflow based on plasma p-tau217 to screen for amyloid β positivity with further confirmatory testing only in uncertain cases. *Nat. Aging* **3**, 1079–1090 (2023).
27. S. E. Schindler *et al.*, Acceptable performance of blood biomarker tests of amyloid pathology–Recommendations from the Global CEO Initiative on Alzheimer's Disease. *Nat. Rev. Neurol.* **20**, 426–439 (2024).
28. A. Corsi, C. Bombieri, M. T. Valenti, M. G. Romanelli, Tau isoforms: Gaining insight into MAPT alternative splicing. *Int. J. Mol. Sci.* **23**, 15383 (2022).
29. S. Janelidze, N. R. Barthélemy, Y. He, R. J. Bateman, O. Hansson, Mitigating the associations of kidney dysfunction with blood biomarkers of Alzheimer disease by using phosphorylated tau to total tau ratios. *JAMA Neurol.* **80**, 516–522 (2023).
30. S. Palmqvist *et al.*, Alzheimer's Association Clinical Practice Guideline on the use of blood-based biomarkers in the diagnostic workup of suspected Alzheimer's disease within specialized care settings. *Alzheimers Dement.* **21**, e70535 (2025).
31. N. Lorius *et al.*, Vascular disease and risk factors are associated with cognitive decline in the Alzheimer disease spectrum. *Alzheimer Dis. Assoc. Disord.* **29**, 18 (2015).
32. J. S. M. Tsui *et al.*, The TREM2 H157Y variant is associated with more severe neurodegeneration in Alzheimer's disease and altered immune-related processes. *Alzheimer's Dement.* **21**, e70586 (2025).
33. Y. Jiang *et al.*, An IL1RL1 genetic variant lowers soluble ST2 levels and the risk effects of APOE-ε4 in female patients with Alzheimer's disease. *Nat. Aging* **2**, 616–634 (2022).
34. P. S. Minhas *et al.*, Restoring hippocampal glucose metabolism rescues cognition across Alzheimer's disease pathologies. *Science* **385**, eabm6131 (2024).
35. Y. Jiang *et al.*, Large-scale plasma proteomic profiling identifies a high-performance biomarker panel for Alzheimer's disease screening and staging. *Alzheimer's Dement.* **18**, 88–102 (2022).
36. Y. Jiang *et al.*, A blood-based multi-pathway biomarker assay for early detection and staging of Alzheimer's disease across ethnic groups. *Alzheimer's Dement.* **20**, 2000–2015 (2024).
37. N. R. Barthélemy, K. Horie, C. Sato, R. J. Bateman, Blood plasma phosphorylated-tau isoforms track CNS change in Alzheimer's disease. *J. Exp. Med.* **217**, e20200861 (2020).
38. D. Bali *et al.*, Comparison of plasma ALZpath p-Tau217 with Lilly p-Tau217 and p-Tau181 in a neuropathological cohort. *Acta Neuropathol. Commun.* **13**, 144 (2025).
39. A. M. Brickman *et al.*, Alzheimer disease blood biomarker concentrations across race and ethnicity groups in middle-aged adults. *JAMA Netw. Open.* **8**, e2545046 (2025).
40. Z. S. Nasreddine *et al.*, The Montreal Cognitive Assessment, MoCA: A brief screening tool for mild cognitive impairment. *J. Am. Geriatr. Soc.* **53**, 695–699 (2005).
41. V. C. Pangman, J. Sloan, L. Guse, An examination of psychometric properties of the Mini-Mental State Examination and the Standardized Mini-Mental State Examination: Implications for clinical practice. *Appl. Nurs. Res.* **13**, 209–213 (2000).
42. X. Robin *et al.*, P roc: An open-source package for R and S+ to analyze and compare ROC curves. *BMC Bioinformatics* **12**, 77 (2011).
43. C. Ginestet, Ggplot2: Elegant graphics for data analysis. *J. R. Stat. Soc. Ser. A Stat. Soc.* **174**, 245–246 (2011).
44. Y. Jiang, W. Zheng, yjiangah/BDpTau217_study. GitHub. https://github.com/yjiangah/BDpTau217_study/. Accessed 10 February 2026.